Stable Fulde-Ferrell-Larkin-Ovchinnikov pairing states in two-dimensional and three-dimensional optical lattices

Zi Cai,[1] Yupeng Wang,[2] and Congjun Wu[1]

[1]*Department of Physics, University of California, San Diego, California 92093, USA*

[2]*Beijing National Laboratory for Condensed Matter Physics, Institute of Physics, Chinese Academy of Sciences, 100080 Beijing, People's Republic of China*

(Received 17 September 2010; revised manuscript received 27 April 2011; published 16 June 2011)

We present the study of the Fulde-Ferrell-Larkin-Ovchinnikov (FFLO) pairing states in the p-orbital bands in both two- and three-dimensional optical lattices. Due to the quasi-one-dimensional band structure which arises from the unidirectional hopping of the orthogonal p orbitals, the pairing phase space is not affected by spin imbalance. Furthermore, interactions build up high-dimensional phase coherence which stabilizes the FFLO states in 2D and 3D optical lattices in a large parameter regime in the phase diagram. These FFLO phases are stable with the imposition of the inhomogeneous trapping potential. Their entropies are comparable to the normal states at finite temperatures.

DOI: 10.1103/PhysRevA.83.063621 PACS number(s): 67.85.−d, 03.75.Ss, 05.30.Fk, 74.20.Fg

The Fulde-Ferrell-Larkin-Ovchinnikov (FFLO) phases are a class of exotic Cooper pairing states exhibiting nonzero center-of-mass momenta [1–4], which occur in spin imbalanced systems with mismatched Fermi surfaces. However, such states are difficult to realize in solid-state systems. The strong orbital effects of external magnetic fields often suppress Cooper pairing before sizable spin polarizations are reached. Moreover, because only small fractions of the mismatched Fermi surfaces can participate pairing, the FFLO states are usually fragile in 2D and 3D systems. In spite of indirect evidence in various heavy fermion compounds and organic superconductors [e.g., $CeCoIn_5$ [5] and λ-(bis(ethylenedithio)tetraselenafulalene)$_2FeCl_4$ [6]], the FFLO states remain elusive.

In the cold atom community, the search for the FFLO pairing states has been attracting considerable interest [7–27]. Spin imbalanced two-component fermion systems have been prepared free of the orbital effects of magnetic fields. However, the problem of the limited pairing phase space remains; thus, phase separations are observed experimentally instead of the FFLO pairing in 3D traps [26,28]. This difficulty is avoided in 1D systems whose Fermi surfaces are points; thus, spin imbalance does not affect the pairing phase space. Considerable progress has been made in quasi-1D systems of coupled optical tubes in Hulet's group [7], in which the partially polarized central regions in the tubes are observed in agreement with the prediction of the Bethe ansatz solution. However, due to the intrinsic strong quantum fluctuations in 1D, the pairing density waves, which are the smoking gun evidence for the FFLO states, cannot be long-range ordered and thus are difficult to observe.

On the other hand, orbital physics with cold atoms in optical lattices has received considerable attention, which gives rise to a variety of new states of matter with both cold bosons and fermions [29–34]. In particular, it has been recently shown that the $p_{x,y}$-orbital band in the honeycomb lattice exhibits different properties from its p_z-orbital counterpart of graphene. These include the strong correlation effects in the flat bands (e.g., Wigner crystallization [35] and ferromagnetism [36]), quantum anomalous Hall states [37], and the heavily frustrated orbital exchange physics [38,39].

In this article, we combine the realization of the FFLO states and the study of orbital physics with cold atoms together. The FFLO states can be stabilized in the p-orbital bands in both 2D square and 3D cubic optical lattices. Different from the metastable p-orbital boson systems [29,34], the p-orbital systems filled with fermions with the fully filled s band are stable due to Pauli's exclusion principle. This work is a natural high-dimensional generalization of the current experiments in Hulet's group [7]. The $p_x(p_y, p_z)$-orbital bands behave like orthogonally crossed quasi-1D arrays due to their highly unidirectional hoppings. The onsite negative Hubbard interactions further build up high-dimensional phase coherence over the entire lattice. Our system combines the advantages of the large pairing phase space of quasi-1D systems and the high-dimensional phase coherence.

The anisotropic p-orbital bands possess the quasi-1D-like structures with perfect nesting at general fillings and spin imbalance. For simplicity, we start with the 2D case. Similar physics applies to the 3D cubic lattice as well. We present the p-band Hamiltonian as

$$H_0 = t_{\parallel} \sum_{\vec{r},\alpha} \{p^{\dagger}_{x,\alpha}(\vec{r}) p_{x,\alpha}(\vec{r}+\hat{e}_x) + p^{\dagger}_{y,\alpha}(\vec{r}) p_{y,\alpha}(\vec{r}+\hat{e}_y)\} - \mu \sum_{\vec{r},\alpha} n_{\alpha}(\vec{r}) - \frac{h}{2} \sum_{\vec{r}} \{n_{\uparrow}(\vec{r}) - n_{\downarrow}(\vec{r})\}, \quad (1)$$

where α refers to spin index, h controls spin imbalance, and $n_{\alpha}(\vec{r}) = p^{\dagger}_{x,\alpha}(\vec{r}) p_{x,\alpha}(\vec{r}) + p^{\dagger}_{y,\alpha}(\vec{r}) p_{y,\alpha}(\vec{r})$ is the particle number of spin α. Only the longitudinal σ-bonding ($t_{\parallel}$) term is kept which describes the hopping between p orbitals along the bond direction as depicted in Fig. 1(a). $t_{\parallel}$ is positive because of the odd parity of the p orbitals. The transverse π-bonding term with the hopping integral $t_{\perp}$ is neglected, which describes the hopping between p orbitals perpendicular to the bond direction as depicted in Fig. 1(b).

In spite of the 2D lattice structure, the p-orbital band structure of Eq. (1) remains quasi-1D-like as depicted in Fig. 2(a). The $p_x(p_y)$-orbital band disperses along the $x(y)$

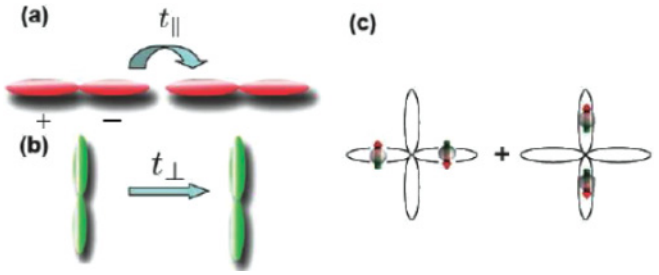

FIG. 1. (Color online) (a) and (b) describe the longitudinal hopping $t_\parallel$ term and the transverse $t_\perp$ term of the the p orbitals, respectively. (c) Pairing hopping term in Eq. (2) locks the phases of two onsite intraorbital pairings in the p_x and p_y orbitals.

direction, respectively, but does not along the $y(x)$ direction. The Fermi surfaces are vertical (p_x) and horizontal (p_y) lines across the entire Brillouin zone. For the arbitrary filling and spin imbalance, the Fermi surfaces of spin-up and -down fermions have the perfect nesting. Consequentially, spin imbalance *does not* suppress the pairing phase volume. The high-dimensional p-orbital systems have the same advantage as that in 1D systems.

The important feature of the 2D p-orbital systems for the FFLO states is that the onsite negative Hubbard interactions build up the 2D phase coherence. The interactions are represented in the standard two-orbital Hubbard model as

$$\begin{aligned} H_{\rm int} = & \sum_{\vec{r}} U[n_{x\uparrow}(\vec{r})n_{x\downarrow}(\vec{r}) + n_{y\uparrow}(\vec{r})n_{y\downarrow}(\vec{r})] \\ & - \sum_{\vec{r}} J[\vec{S}_x(\vec{r})\cdot\vec{S}_y(\vec{r}) - \frac{1}{4}n_x(\vec{r})n_y(\vec{r})] \\ & + \sum_{\vec{r}} \Delta[p^\dagger_{x\uparrow}(\vec{r})p^\dagger_{x\downarrow}(\vec{r})p_{y\downarrow}(\vec{r})p_{y\uparrow}(\vec{r}) + \text{H.c.}], \end{aligned} \tag{2}$$

where $U = g\int dr|\psi_{p_{x,y}}(\vec{r})|^4 < 0$ and g is the contact interaction in the s-wave scattering approximation. J and Δ satisfy $J = \frac{2U}{3} < 0$ and $\Delta = \frac{U}{3} < 0$ [36]. The negative U term gives

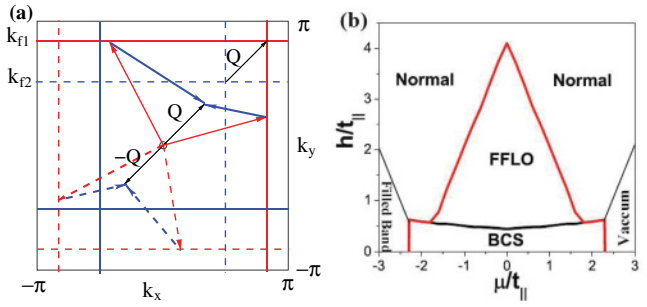

FIG. 2. (Color online) (a) Nesting of the p-orbital Fermi surfaces ensures that all of the Fermi surfaces are paired at a general filling and spin imbalance. The Fermi surfaces of the p_x (p_y) orbitals are vertical (horizontal) lines; those of the majority (minority) spins are marked red (blue). Fermi surfaces marked with solid (dashed) lines are paired with the center-of-mass momentum $\pm\vec{Q}$, respectively. The red and blue arrows represents the Fermi wave vectors of spin-up and -down fermions participating in Cooper pairing. (b) 2D phase diagram from the B-de G solution as chemical potential μ and the magnetic field h with $U/t_\parallel = -1.5$.

rise to the dominant intraorbital singlet pairings in the p_x and p_y orbitals, defined as

$$\begin{aligned} \Delta_x(\vec{r}) &= \langle G|p_{x\uparrow}(\vec{r})p_{x\downarrow}(\vec{r})|G\rangle, \\ \Delta_y(\vec{r}) &= \langle G|p_{y\uparrow}(\vec{r})p_{y\downarrow}(\vec{r})|G\rangle, \end{aligned} \tag{3}$$

where $|G\rangle$ is the mean-field pairing ground states. The J term induces the interorbital singlet pairing between p_x and p_y orbitals. However, because the Fermi surfaces of p_x and p_y orbitals are orthogonal, the interorbital pairing is unfavorable.

The pair hopping Δ term in Eq. (2) can be considered as the internal Josephson coupling to lock the phases of two intraorbital pairings Δ_x and Δ_y. As a result, the motion of Cooper pairs are 2D-like in spite of the quasi-1D-like single fermion hopping. To clarify the pairing symmetry, we first consider two fermions on the same site to gain some intuition. The s-wave Feshbach resonances forbid a spin triplet channel and induce a spin singlet pairing. In the spin singlet channel, their orbital wave functions are symmetric as $p_x^2 + p_y^2$, $p_x^2 - p_y^2$, and $p_x p_y$, respectively. The first one has energy $U + \Delta = 4U/3$, while the later two are degenerate with energy $U - \Delta = J = 2U/3$. From this simple analysis, we can see that the system favors pairing with $p_x^2 + p_y^2$ orbital symmetry [as shown in Fig. 1(c)], while pairing with the other two symmetries are suppressed, which can be verified by the numerical results below.

We have performed calculations based on the self-consistent Bogoliubov-de Gennes (B-deG) solution to study the competition among the FFLO state, the BCS state, and the normal state as presented in Fig. 2(b). To synchronize the phases of $\Delta_x(\vec{r})$ and $\Delta_y(\vec{r})$ on each site, their center-of-mass wave vectors in the FFLO states have to be the same. This can be achieved by choosing the pair density wave vectors along the diagonal direction $\pm\vec{Q}$ defined as $\vec{Q} = (\delta k_f, \delta k_f)$, where $\delta k_f = k_{f_1} - k_{f_2}$, and $k_{f_{1,2}}$ are Fermi wave vectors of the majority and minority spins, respectively, as indicated in Fig. 2(a). By the symmetry of the square lattice, $\vec{Q}' = \pm(\delta k_f, -\delta k_f)$ is another possible choice of the pair density wave vector. We consider the simplest Larkin-Ovchinnikov (LO) states with one pair of Cooper pair momenta $\pm\vec{Q}$, with the sinusoidal order parameter configuration as

$$\Delta_x(\vec{r}) = \Delta_y(\vec{r}) = |\Delta|\cos(\vec{Q}\cdot\vec{r}). \tag{4}$$

The LO state breaks both translational and the fourfold lattice rotational symmetries. We have performed unbiased real-space B-de G calculations without specifying the FFLO momentum in the initial conditions but rather starting from a configuration with uniform pairing. The FFLO momentum Q in the above analysis is obtained when the numerical convergence has arrived. Compared with the phase diagram of spin-imbalanced fermions in the s-orbital band, the FFLO phase in our p-orbital band system exists in a much larger regime in the phase diagram sandwiched between the fully paired BCS phase and the fully polarized normal phase.

Next, we study a more realistic situation: the effects of the soft confining potential on the p-orbital FFLO states, by performing self-consistent real-space B-de G calculations. We consider a 30×30 lattice with the harmonic trapping potential $V_{\rm ex} = A(r/a)^2$ where $A/t_\parallel = 5 \times 10^{-3}$, r is the

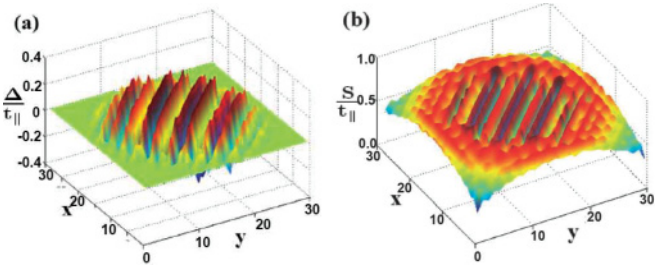

FIG. 3. (Color online) B-de G solution of the p-orbital FFLO state in a 30×30 lattice with a weak confining trap. (a) Order parameter distribution of $\Delta_x(\vec{r})$ oscillates along the $[\bar{1}1]$ direction. (b) Spin density distribution $S_z(\vec{r})$ peaks around the gap nodes.

distance from the trap center, and a is the lattice constant. The real-space distribution of order parameter $\Delta_x(\vec{r})$ is shown in Fig. 3(a) with the parameters chosen as $h/t_\parallel = 3$, $U/t_\parallel = -3$, and $\mu = 0$. Clearly Δ_x oscillates along the $[\bar{1}1]$ direction in agreement with the previous analysis. To verify Eq. (4), we further calculate the difference between the pairing orders in different orbitals. In the bulk, the relation that $\Delta_x(\vec{r}) = \Delta_y(\vec{r})$ is well satisfied. The difference between $\Delta_x(\vec{r})$ and $\Delta_y(\vec{r})$ is only important at the boundary which breaks the symmetry between the p_x and p_y orbitals. The spin-density distribution $s_z(\vec{r}) = n_\uparrow(\vec{r}) - n_\downarrow(\vec{r})$ is depicted in Fig. 3(b). It peaks around the gap nodes, which is consistent with the fact that spin polarization suppresses Cooper pairing.

Next we discuss the effect of the small π-bonding $t_\perp$, which has been neglected above but always exists in realistic systems. The $t_\perp$ term restores the 2D nature of the Fermi surfaces and suppresses the perfect nesting; therefore, it is harmful to the FFLO states. Our numerical result indicates that the FFLO state remains stable at small values of $t_\perp$. For example, with $U/t_\parallel = -3$, $h/t_\parallel = 3$, and $\mu = 0$, the FFLO state survives until $t_\perp/t_\parallel$ reaches 0.12. Beyond this value, it changes to the normal state through a first-order phase transition. As calculated in Ref. [30], with the optical potential depth $V_0/E_R \approx 15$, $t_\parallel$ is at the order of $0.1E_R$ and $t_\perp/t_\parallel \approx 5\%$. Increasing optical potential depth further suppresses $t_\perp$; thus, there is a large parameter regime to stabilize the FFLO states.

The physics of the FFLO states in the p-orbital bands in the 3D cubic optical lattices is similar. The 3D p-orbital Hamiltonian is similar to Eqs. (1) and. (2), and further augmented by a new orbital p_z. The pair density wave vectors are along the body diagonal directions, i.e., the $\pm[111]$ or other equivalent directions. Similar to the Eq. (4), the FFLO state in the 3D cubic optical lattice is characterized by the sinusoidal order parameter configuration as

$$\Delta_x(\vec{r}) = \Delta_y(\vec{r}) = \Delta_z(\vec{r}) = |\Delta| \cos(\vec{Q} \cdot \vec{r}). \tag{5}$$

where $\vec{Q} = (\pm\delta k_f, \pm\delta k_f, \pm\delta k_f)$ are along the body-diagonal directions.

In the 3D p-orbital bands, the long-range ordered BCS and FFLO states survive at finite temperatures, and mean-field theory works qualitatively well. We present the finite temperature phase diagram of the competing orders at $U/t_\parallel = -2.4$ and $\mu = 0$ in Fig. 4(a). The FFLO state can also survive to finite critical temperatures at the same order of T_c. We further present the entropy S vs h for different competing

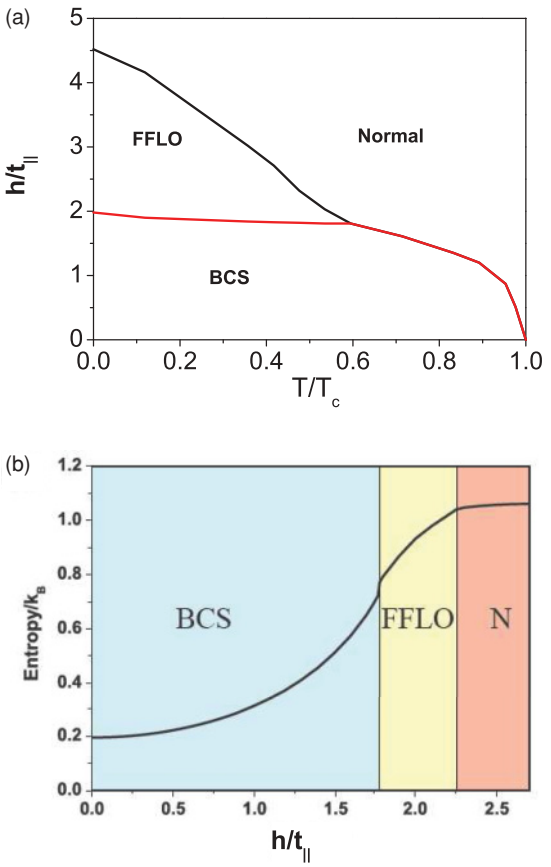

FIG. 4. (Color online) (a) Finite temperature phase diagram for the 3D p-orbital bands with $U/t_\parallel = -2.4$ and $\mu = 0$. $T_c/t_\parallel = 0.84$ is the critical temperature for the BCS state. (b) Entropy density S/k_B vs $h/t_\parallel$ at a finite temperature of $T/t_\parallel = 0.4$ with parameters $\mu = 0$ and $U/t_\parallel = -2.4$.

orders at a fixed temperature $T/t_\parallel = 0.4$ in Fig. 4(b). The FFLO state has a large value of entropy density due to the extra unpaired majority fermions, which interpolate between the BCS and the fully polarized normal state. This greatly increases the accessibility of the FFLO state in the cold atom optical lattices. The transition between the BCS and the FFLO states is of the first order as indicated by the discontinuity of entropy in Fig. 4(b).

At last, we discuss experimental realizations and detections. The p-band fermion systems can be realized by first preparing a large enough number of atoms to fully fill the s-orbital band; thus, the extra particles will fill the p bands. The attractive interaction can be achieved through Feshbach resonances in lattices [7,40], whose strength can be tuned to a value that is comparable to the band width of $4t_\parallel \approx 0.5E_R$ at $V_0/E_R \approx 15$ [30], but is still small compared to band gaps which are around several E_R. Our work predicts a large stable parameter regime for the FFLO states. These states can be detected by many methods [21,23,24], such as the direct imaging of the density profile oscillations of each of the fermion components, the rf spectroscopy measurement on the collective modes, converting Cooper pairs into molecules and measuring their momenta, the shot-noise correlation of the Fermi momenta between $\vec{k}$ and $-\vec{k} \pm \vec{Q}$, etc. In particular, the recent development of the *in situ* imaging methods with the single site resolution [41,42]

can be used to accurately determine the spatial oscillation of the FFLO states.

In summary, we have studied the competing orders among the FFLO, the BCS, and the normal states in the spin imbalanced p-orbital band systems in both 2D and 3D. The FFLO states are stabilized by the combined effects of the quasi-1D Fermi surfaces and the high-dimensional phase coherence built up by the interorbital interactions. The pairing density wave vectors are along the diagonal directions to facilitate the maximal interorbital pairing phase coherence. The FFLO states are robust with many realistic experimental effects including the confining trap, the small transverse π bonding, and finite temperatures. It would be nice to realize the 2D and 3D stable FFLO phases in the p-orbital bands in optical lattices which have not been identified in solid-state systems yet.

Z.C. and C.W. are supported by the Sloan Research Foundation, NSF-DMR-03-42832, and AFOSR-YIP. Y.P.W. is supported by the NSFC and 973-Project of MOST (China).

[1] P. Fulde and R. A. Ferrell, Phys. Rev. **135**, A550 (1964).
[2] A. I. Larkin and Y. N. Ovchinnikov, Sov. Phys. JETP **20**, 762 (1965).
[3] R. Casalbuoni and G. Nardulli, Rev. Mod. Phys. **76**, 263 (2004).
[4] Y. Matsuda and H. Shimahara, J. Phys. Soc. Jpn. **76**, 051005 (2007).
[5] H. A. Radovan *et al.*, Nature (London) **425**, 51 (2003); A. Bianchi, R. Movshovich, C. Capan, P. G. Pagliuso, and J. L. Sarrao, Phys. Rev. Lett. **91**, 187004 (2003); K. Kakuyanagi, M. Saitoh, K. Kumagai, S. Takashima, M. Nohara, H. Takagi, and Y. Matsuda, *ibid.* **94**, 047602 (2005).
[6] S. Uji, H. Shinagawa, T. Terashima, T. Yakabe, Y. Terai, M. Tokumoto, A. Kobayashi, H. Tanaka, and H. Kobayashi, Nature (London) **410**, 908 (2001).
[7] Y. Liao, A. S. C. Rittner, T. Paprotta, W. H. Li, G. B. Partridge, R. G. Hulet, S. K. Baur, and E. J. Mueller, Nature (London) **467**, 567 (2010).
[8] W. Ketterle and M. W. Zwierlein, e-print arXiv:0801.2500.
[9] Y. L. Loh and N. Trivedi, Phys. Rev. Lett. **104**, 165302 (2010).
[10] E. Zhao and W. V. Liu, Phys. Rev. A **78**, 063605 (2008).
[11] T. K. Koponen, T. Paananen, J. P. Martikainen, and P. Törmä, Phys. Rev. Lett. **99**, 120403 (2007).
[12] T. K. Koponen, T. Paananen, J. P. Martikainen, M. R. Bakhtiari, and P. Törmä, New J. Phys. **10**, 045014 (2008).
[13] M. M. Parish, S. K. Baur, E. J. Mueller, and D. A. Huse, Phys. Rev. Lett. **99**, 250403 (2007).
[14] A. E. Feiguin and F. Heidrich-Meisner, Phys. Rev. B **76**, 220508 (2007).
[15] G. G. Batrouni, M. H. Huntley, V. G. Rousseau, and R. T. Scalettar, Phys. Rev. Lett. **100**, 116405 (2008).
[16] J. M. Edge and N. R. Cooper, Phys. Rev. Lett. **103**, 065301 (2009).
[17] X.-J. Liu, H. Hu, and P. D. Drummond, Phys. Rev. A **76**, 043605 (2007).
[18] T. Paananen, T. K. Koponen, P. Törmä, and J. P. Martikainen, Phys. Rev. A **77**, 053602 (2008).
[19] A. Lüscher, R. M. Noack, and A. M. Läuchli, Phys. Rev. A **78**, 013637 (2008).
[20] P. Kakashvili and C. J. Bolech, Phys. Rev. A **79**, 041603 (2009).
[21] K. Yang, Phys. Rev. Lett. **95**, 218903 (2005).
[22] J. Kinnunen, L. M. Jensen, and P. Törmä, Phys. Rev. Lett. **96**, 110403 (2006).
[23] T. Mizushima, K. Machida, and M. Ichioka, Phys. Rev. Lett. **94**, 060404 (2005).
[24] M. R. Bakhtiari, M. J. Leskinen, and P. Törmä, Phys. Rev. Lett. **101**, 120404 (2008).
[25] P. Nikolić, A. A. Burkov, and A. Paramekanti, Phys. Rev. B **81**, 012504 (2010).
[26] G. B. Partridge, W. Li, Y. A. Liao, R. G. Hulet, M. Haque, and H. T. C. Stoof, Phys. Rev. Lett. **97**, 190407 (2006).
[27] L. Radzihovsky and D. E. Sheehy, Rep. Prog. Phys. **73**, 076501 (2010).
[28] M. W. Zwierlein *et al.*, Nature (London) **442**, 54 (2006).
[29] T. Muller, S. Folling, A. Widera, and I. Bloch, Phys. Rev. Lett. **99**, 200405 (2007).
[30] A. Isacsson and S. M. Girvin, Phys. Rev. A **72**, 053604 (2005).
[31] W. V. Liu and C. Wu, Phys. Rev. A **74**, 13607 (2006).
[32] A. B. Kuklov, Phys. Rev. Lett. **97**, 110405 (2006).
[33] V. M. Stojanović, C. Wu, W. V. Liu, and S. Das Sarma, Phys. Rev. Lett. **101**, 125301 (2008).
[34] G. Wirth, M. Ölschläger, A. Hemmerich, Nat. Phys. **7**, 147153 (2011).
[35] C. Wu, D. Bergman, L. Balents, and S. Das Sarma, Phys. Rev. Lett. **99**, 070401 (2007).
[36] S. Z. Zhang, H. H. Hung, and C. Wu, Phys. Rev. A **82**, 053618 (2010).
[37] M. Zhang, H. H. Hung, C. W. Zhang, and C. Wu, Phys. Rev. A **83**, 023615 (2011).
[38] C. Wu, Phys. Rev. Lett. **100**, 200406 (2008).
[39] G. Chern and C. Wu, e-print arXiv:1104.1614v2.
[40] J. K. Chin, D. E. Miller, Y. Liu, C. Stan, W. Setiawan, C. Sanner, K. Xu, and W. Ketterle, Nature (London) **443**, 961 (2006).
[41] N. Gemelke, X. Zhang, C. Hung, and C. Chin, Nature (London) **460**, 995 (2009).
[42] W. S. Bakr, J. I. Gillen, A. Peng, S. Fölling, and M. Greiner, Nature (London) **462**, 74 (2009).